Resonance Hyper-Raman Spectra of Zinc Phthalocyanine

Weinan Leng and Anne Myers Kelley*

School of Natural Sciences, University of California, Merced, P.O. Box 2039, Merced, California 95344

Received: February 3, 2008; Revised Manuscript Received: April 14, 2008

Hyper-Raman spectra were obtained for zinc phthalocyanine in a dilute pyridine solution at excitation wavelengths that are two-photon resonant with the one-photon-allowed B band (360−380 nm) as well as with the two-photon absorption near 440 nm reported by Drobizhev et al. (*J. Chem. Phys.* 2006, *124*, 224701). In both regions, the hyper-Raman spectra were very different from the linear resonance Raman spectra at the corresponding excitation frequencies. While the resonance Raman spectra show only *g* symmetry modes, almost all of the hyper-Raman frequencies can be assigned as fundamentals of E_u symmetry that also are observed in the infrared absorption spectrum or E_u symmetry combination bands. These results contrast sharply with previous observations of highly noncentrosymmetric push−pull conjugated molecules and are consistent with a structure for phthalocyanine in solution that is centrosymmetric or nearly so. The hyper-Raman spectra show different intensity patterns in the two excitation regions, consistent with different Franck−Condon and/or vibronic coupling matrix elements for the different resonant states.

Introduction

Hyper-Raman scattering is the two-photon analogue of ordinary Raman scattering: two photons from the excitation source are destroyed, and a scattered photon is created whose frequency is shifted from the second harmonic by one or more quanta of ground-state vibrational modes. When there are no intermediate electronic resonances, hyper-Raman scattering is typically a very weak process that is often obscured by competing nonlinear processes in liquids.[1,2] We have shown that hyper-Raman scattering can be quite strong when the excitation is two-photon resonant with an electronic excitation of a donor−acceptor push−pull conjugated molecule that is both highly polar and highly polarizable.[3–11] In such molecules, there are no symmetry restrictions to prevent a given excited state from being simultaneously one- and two-photon-allowed, and it is the existence of such low-lying states that gives these molecules their large hyperpolarizabilities as manifested by strong hyper-Rayleigh scattering. The dominant source of hyper-Raman scattering, when excited on resonance with these electronic states, is the A-term, in which the vibrational excitation accompanies fully allowed electronic transitions.[2] The matrix elements are then products of purely electronic transition moments and vibrational Franck−Condon factors, and the intensity patterns in the hyper-Raman spectra provide the same type of information about the simultaneously one- and two-photon-allowed resonant electronic states that ordinary resonance Raman spectra provide for strongly one-photon-allowed states.[5,12,13]

The situation should be very different when the molecule of interest has a center of symmetry. In this case, the three-photon transition involved in hyper-Raman scattering must cause a change in parity, meaning that the process must excite a *u* symmetry vibration.[2] In the context of resonance enhanced scattering, either the two-photon (absorbing) or the one-photon (emitting) electronic transition must be vibronically induced. Hyper-Rayleigh scattering should, in principle, be absent in a centrosymmetric molecule.

Phthalocyanines and porphyrins are interesting classes of molecules that are nominally centrosymmetric, or nearly so, and have strong electronic absorbances. In general, the linear absorption spectra of phthalocyanines feature a strong, sharp Q band in the 600−700 nm region and a much broader B band near 350 nm. Excitation that is two-photon resonant with the B band also will be preresonant with the Q band, which should enhance some of the pathways leading to hyper-Raman scattering (although see ref 11). Centrosymmetric porphyrins, in contrast, have a very strong B (Soret) band and a Q band that is generally much weaker and blue-shifted relative to that of phthalocyanines. The latter are therefore more promising candidates for interesting multiple-resonance effects. In addition, Drobizhev et al.[14] measured the two-photon absorption spectra of a number of phthalocyanines through the two-photon-excited fluorescence method and identified resonances slightly to the red of the B band, which they attributed to one-photon-forbidden, purely electronic $g-g$ transitions. Hyper-Raman scattering should be a useful tool for confirming the presence of those states and exploring their structures.

Experimental Procedures

Zn-29*H*,31*H*-phthalocyanine (ZnPc) was purchased from Aldrich and used as received. Pyridine (Fluka) was dried over 3 Å molecular sieves. Solutions for Raman and hyper-Raman spectroscopy were prepared in pyridine at a concentration of ∼0.23 mM. Absorption spectra were recorded on a Hitachi 3010-U UV−vis spectrophotometer. Resonance hyper-Raman (RHR) and resonance Raman (RR) spectra were measured using excitation from the fundamental and second harmonic, respectively, of an unamplified picosecond Ti:sapphire laser. The scattering was collected at 90°, dispersed with a 0.5 m single spectrograph, and detected with a liquid nitrogen cooled CCD. The experimental setup is described in more detail in refs 4and 6.

Results

ZnPc has its Q band maximum at about 670 nm. The B band maximum is near 350 nm, but it extends to wavelengths beyond

* Corresponding author. E-mail: amkelley@ucmerced.edu.

10.1021/jp801016q CCC: $40.75
Published on Web 06/07/2008

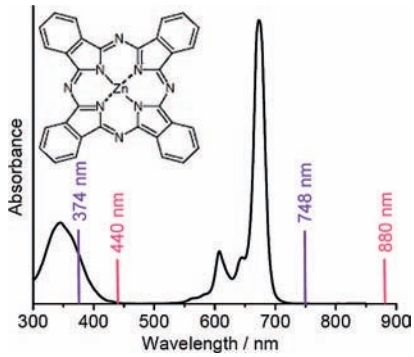

Figure 1. Linear absorption spectrum of ZnPc in pyridine and two pairs of the one- and two-photon wavelengths used in this work.

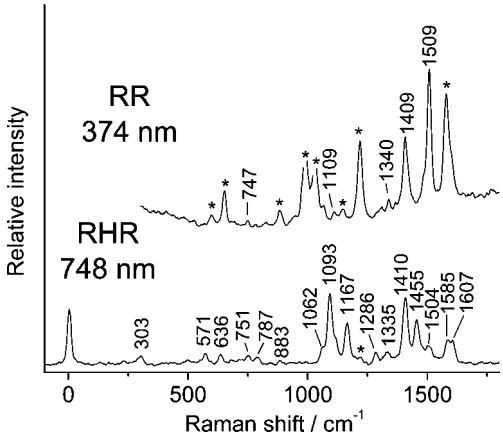

Figure 2. RR and RHR spectra of ZnPc in pyridine at the indicated excitation wavelengths. The RR spectrum is displaced vertically and scaled. Asterisks mark solvent peaks. The hyper-Rayleigh peak (0 cm^{-1}) in the RHR spectrum also originates mainly from the solvent.

400 nm. Our Ti:sapphire laser source can easily reach two-photon resonance with the B band but cannot quite have a simultaneous one-photon resonance with the Q band. The one-photon absorption spectrum is shown in Figure 1.

When dissolved in pyridine at 0.23 mM and excited at 748/374 nm, ZnPc exhibits reasonably strong resonance Raman scattering and readily detectable hyper-Raman scattering (Figure 2). Interestingly, pyridine itself exhibits measurable nonresonant hyper-Raman intensity in one line near 1220 cm^{-1}, unlike any of the other solvents we have used in other studies. This line is also the strongest one reported in the 1064 nm excited hyper-Raman spectrum of liquid pyridine by Johnson et al.[15] The hyper-Rayleigh scattering of ZnPc/pyridine solutions is weak and nearly independent of ZnPc concentration, indicating that most of it comes from the solvent. We estimate that the hyper-Rayleigh scattering of ZnPc is less than half the intensity of the strongest hyper-Raman line when excited at 748 nm. The RR and RHR spectra of ZnPc show almost no correspondence. Both of these observations are consistent with ZnPc retaining its center of symmetry or nearly so, with *g* modes active in RR and *u* modes active in RHR.

At excitation wavelengths longer than 400/800 nm, resonant with the two-photon transition identified by Drobizhev et al.,[14] the RR spectra are much weaker than those obtained at the shorter excitation wavelengths. The lines at 1409 and 1509 cm^{-1} dominate the RR spectra at both excitation wavelengths, but the line at 747 cm^{-1}, in particular, has a considerably greater relative intensity at 440 nm than at 374 nm. The hyper-Raman scattering from ZnPc with excitation wavelengths in the 800−880 nm region also is quite weak. Long accumulation

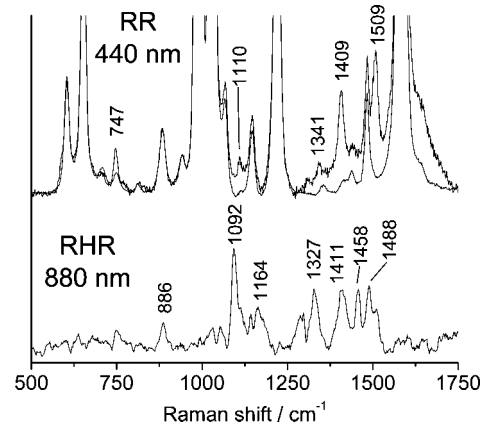

Figure 3. RR and RHR spectra of ZnPc in pyridine at the indicated excitation wavelengths. The RR spectrum is displaced vertically and scaled and is superimposed on the Raman spectrum of the pyridine solvent to show weak ZnPc lines that overlap pyridine lines.

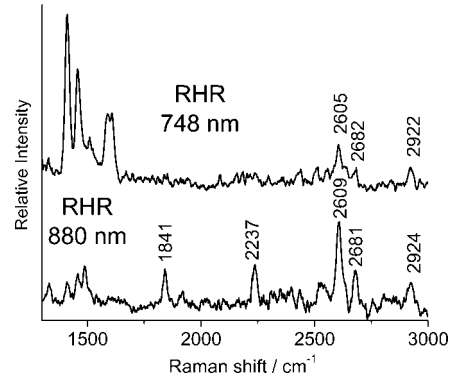

Figure 4. Overtone and combination band region of RHR spectra of ZnPc at 748 and 880 nm excitation. Accumulation times are 75 min at 880 nm and 20 min at 748 nm.

times were required to obtain reasonable spectra in this excitation region (~75 min for the 880 nm excited spectra, as compared to 20 min with 748 nm excitation). Figure 3 compares the RR and RHR spectra at a two-photon wavelength of 440 nm. All of the peaks that are labeled in the RHR spectrum were clearly observed in each of four independent scans taken on different days and with different settings of the detection window.

Figure 4 shows the weak overtone region of the RHR spectra in both excitation regions. The 748 nm excited RHR spectra exhibit lines at 2605, 2681, and 2922 cm^{-1}, which can be assigned as E_u symmetry combination bands of the three strongest fundamentals in the RHR spectrum (1092, 1167, and 1412 cm^{-1}) plus the strongest line in the RR spectrum (1509 cm^{-1}). The 880 nm excited spectra show these same three lines plus several others, the strongest being at 1841 and 2237 cm^{-1}. These also have likely assignments as a RR fundamental plus a RHR fundamental, 1841 = 747 + 1092 and 2237 = 747 + 1488. In addition, the strongest lines in the overtone and combination band region are considerably stronger than the fundamentals in the 880 nm excited spectrum, while they are considerably weaker in the 748 nm spectrum. The RR spectra show no lines in the overtone region that cannot be attributed to the pyridine solvent. Evidently, the RR overtones and combination bands of ZnPc are quite weak.

Discussion

The Q band absorption of ZnPc in pyridine shows a strong, sharp electronic origin plus weak vibronic bands at ~650 and

TABLE 1: Observed Resonance Raman and Resonance Hyper-Raman Frequencies in Fundamental Region for ZnPc in Pyridine, Experimental IR and Nonresonant Raman Frequencies,[21] and Assignments Based on DFT Calculations[22]

exptl RR frequency (cm^{-1})		exptl RHR frequency (cm^{-1})				DFT calculations	
374 nm	440 nm	748 nm	880 nm	exptl Raman frequency (cm^{-1})	exptl IR frequency (cm^{-1})	frequency (cm^{-1})	symmetry
		303				295	E_u
		571			571	562	E_u
		636			634	627	E_u
747	747			747		735	B_{1g}
		751			752	739	E_u
		787			780	786	E_u
		883	886		878/887	871	E_u
		1062			1060	1046	E_u
		1093	1092		1088	1090	E_u
1109	1110			1109		1111	A_{1g}
		1167	1164		1173	1174	E_u
		1286			1284	1310	E_u
		1335	1327		1332	1331	E_u
1340	1341			1340		1334/1341	A_{1g}/B_{1g}
1409	1407			1406		1386/1413	A_{1g}/A_{1g}
		1410	1411		1409	1400	E_u
		1455	1458		1453	1453	E_u
			1488		1483	1477	E_u
		1504					
1509	1508			1505		1491/1529	A_{1g}/B_{1g}
		1585			1586	1574	E_u
		1607			1607	1598	E_u

~1600 cm^{-1}. The B band region is much broader and shows no clear vibronic structure in room-temperature pyridine solutions. Previous experimental studies using absorption and magnetic circular dichroism spectroscopy have assigned the B band absorption to two or more electronic transitions.[16–18] Time-dependent density functional theory calculations[19] assign the Q band absorption to a single transition of ^1E_u symmetry dominated by the HOMO ($2a_{1u}$) to LUMO ($7e_g$) excitation, while at least three different transitions of ^1E_u symmetry, all dominated by excitations from different occupied orbitals to the LUMO, contribute significantly to one-photon absorption in the B band region. The TDDFT calculations[19] did not specifically address two-photon excitations, but the reported orbital energies suggest a two-photon state of B_{1g} symmetry near 22 420 cm^{-1} (446 nm) arising from the HOMO ($2a_{1u}$) to LUMO + 1 ($3b_{1u}$) excitation.

Several groups have presented vibrational frequency and normal mode calculations for ZnPc. Ding et al. reported semiempirical (PM3) calculations under the assumption of D_{4h} symmetry.[20] A slightly later study by Tackley et al. using density functional theory with the 6-31G(d,p) basis and the RBLYP functional[21] found an imaginary frequency when the geometry was constrained to D_{4h}. Relaxing that constraint yielded a minimum at a C_{4v} geometry that has the Zn slightly out of the plane of the ring and some slight doming of the phthalocyanine. Very recently, Liu et al. also reported a DFT study on ZnPc using the 6-31G(d) basis set and the B3LYP functional.[22] They reported no imaginary frequencies when the geometry was constrained to planar D_{4h}. It is not clear as to why the two groups using DFT methods obtained different equilibrium geometries; however, under the assumption that the deviation from D_{4h} symmetry is at most minor, we base our analysis on the D_{4h} normal mode frequencies and descriptions. In D_{4h}, ZnPc has 165 normal modes distributed as $8A_{2u} + 56E_u + 14A_{1g} + 14B_{1g} + 14B_{2g} + 26E_g + 13A_{2g} + 6A_{1u} + 7B_{1u} + 7B_{2u}$. A_{1g}, B_{1g}, and B_{2g} are Raman-allowed in-plane modes, E_g are Raman-allowed out-of-plane modes, E_u are IR-allowed in-plane, and A_{2u} are IR-allowed out-of-plane. As only the in-plane vibrations should be strongly enhanced by resonance with $\pi-\pi^*$ electronic transitions, we would expect to see only A_{1g}, B_{1g}, and/or B_{2g} modes in the Raman spectrum. If the in-plane tensor components are assumed to dominate the hyperpolarizability, the E_u modes are the only ones that are hyper-Raman-allowed regardless of resonance condition.[23]

Table 1 summarizes the vibrations observed in the RR and RHR spectra and gives the most likely assignments to the calculated frequencies of Liu et al.[22] The five lines clearly observed in the ZnPc resonance Raman spectra (747, 1109, 1340, 1408, and 1509 cm^{-1}) correspond to lines previously reported in the FT-Raman spectrum.[21] Most of these lines can reasonably be assigned as either A_{1g} or B_{1g} modes, although only the B_{1g} assignment appears likely for the 747 cm^{-1} mode. Excitation rigorously on resonance with a strongly allowed electronic transition usually excites mainly the totally symmetric modes that obtain their intensity through Franck−Condon activity, although nontotally symmetric modes also may acquire significant intensity through Herzberg−Teller coupling. In general, the Franck−Condon (A-term) intensity falls off more rapidly with detuning away from resonance than does the vibronically induced (B-term) intensity. The assignment of the 747 cm^{-1} mode as a B_{1g} fundamental is consistent with the greater relative prominence of this line in the less intense, 440 nm excited (preresonant) RR spectrum as compared to the fully resonant, 374 nm excited spectrum.

All of the frequencies observed in the fundamental region of the RHR spectrum correspond well to E_u modes seen in the IR spectrum except for the one at 303 cm^{-1}, which lies outside the frequency range of the IR experiments, and the one at 1504 cm^{-1}. The closeness in frequency between the 1504 cm^{-1} RHR mode and the 1508 cm^{-1} RR mode is probably accidental (i.e., they are not the same mode), but there is no line near this frequency in the IR spectrum, and the RHR mode is not readily assignable as any E_u symmetry fundamental. It is not a very strong line in the RHR spectrum but is clearly observable at 748 nm excitation (Figure 2) and appears to be present at 880 nm as well (Figure 3). It is most likely a combination band of E_u symmetry, but a specific assignment is not possible at present.

Following Chung and Ziegler[24] and Bonang and Cameron,[25] the leading vibronic term yielding RHR intensity in centrosymmetric molecules, the B-term, can be written as follows:

$$B = \sum_{a} \sum_{sn,m} \left\{ \frac{M_{ge}^{0} \langle f|m\rangle [M_{es}^{a'} M_{sg}^{0} \langle m|Q_a|n\rangle \langle n|0\rangle + M_{es}^{0} M_{sg}^{a'} \langle m|n\rangle \langle n|Q_a|0\rangle]}{(\nu_{sn} - \nu_L)(\nu_{em} - 2\nu_L - i\Gamma)} + \frac{M_{ge}^{a'} M_{es}^{0} M_{sg}^{0} \langle f|Q_a|m\rangle \langle m|n\rangle \langle n|0\rangle}{(\nu_{sn} - \nu_L)(\nu_{em} - 2\nu_L - i\Gamma)} \right\} \quad (1)$$

This equation assumes a single two-photon-resonant electronic state e, which has vibrational sublevels m. The 0 and f label the initial and final vibrational levels of ground electronic state g in the hyper-Raman process, and s labels all possible intermediate electronic states in the two-photon upward process with vibrational sublevels n. M_{ij}^{0} is the purely electronic transition moment between states i and j, while $M_{ij}^{a'}$ is the derivative of the $i \rightarrow j$ transition moment along antisymmetric vibrational mode Q_a. ν_L is the laser frequency, which is assumed to be far from resonance with any intermediate-state resonance ν_{sn} but near or within two-photon resonance with ν_{em}. Thus, the leading term in the RHR intensity involves two fully allowed electronic transitions and one that is vibronically induced. The first term of eq 1 combines a vibronically induced upward two-photon transition with a fully allowed downward one-photon transition and is expected to dominate when the excitation is two-photon resonant with the one-photon-allowed B band. The second term in eq 1 represents a fully allowed two-photon upward transition combined with a vibronically induced one-photon emissive transition and should dominate when the excitation frequency is resonant with the longer wavelength one-photon forbidden, two-photon-allowed transition. In either case, because different potential energy surfaces cannot be displaced along a nontotally symmetric vibrational mode, the presence of matrix elements including a nontotally symmetric normal mode ($\langle i|Q_a|j\rangle$) requires that the final vibrational state f contain one quantum of the nontotally symmetric mode Q_a; it may or may not also be excited in totally symmetric modes depending on the Franck−Condon activity in these modes. Therefore, regardless of which resonance condition exists, we expect to observe fundamentals of E_u modes and combination bands involving these modes. All of the combination bands we observe are assignable in this manner.

Our observation of only g symmetry modes in the RR and (with the possible exception of the 1504 cm^{-1} line) only u symmetry modes in the RHR spectrum of ZnPc is consistent with expectations for a centrosymmetric structure and with the reported RHR spectrum of CS_2 vapor.[24] However, totally symmetric A_g modes were reported in the RHR spectrum of naphthalene,[25] a number of g symmetry modes were identified in the RHR spectrum of C_{60},[26] and the RHR spectrum of a symmetrically substituted distyrylbenzene was nearly identical to the RR spectrum despite the presence of a nominal center of symmetry.[27] All of these spectra were obtained in fluid solution, and it is not clear whether the activity of nominally g symmetry modes reflects symmetry breaking through a locally asymmetric solvation environment or arises from alternative scattering mechanisms such as magnetic dipole transitions.[26]

Figure 5 indicates the most likely paths through state space for the processes of resonance Raman scattering, hyper-Raman on resonance with the two-photon g symmetry T state, and hyper-Raman on resonance with the one-photon B state. As the B state is strongly electronically allowed, we expect that the dominant source of RR enhancement is the A-term (Franck−Condon activity in displaced totally symmetric modes). The Q band transition is also strongly electronically allowed from the ground state and shows very weak Franck−Condon activity in any mode, so we expect that the vibrationless $0 \rightarrow Q$ transition should dominate the first radiation−matter interaction in the hyper-Raman process. When the two-photon resonant state is the B state, the $Q \rightarrow B$ transition is electronically forbidden and must be vibronically induced by a u symmetry vibration; the $B \rightarrow 0$ transition can then occur either with no further vibrational excitation, giving rise to u symmetry fundamentals, or with excitation of one of the RR active modes, giving rise to $g + u$ combination bands. When the two-photon resonant state is the two-photon T state, the $Q \rightarrow T$ transition is electronically allowed and can occur either without vibrational excitation or with excitation of a vibration that is Franck−Condon-allowed in the $Q \rightarrow T$ transition; the $T \rightarrow 0$ transition then must be vibronically induced, again giving rise to either u symmetry fundamentals or $g + u$ combination bands.

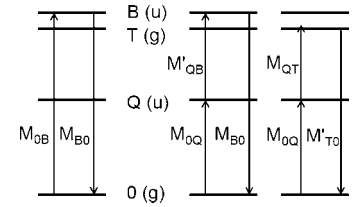

Figure 5. Expected dominant pathways for RR scattering (left), RHR on resonance with u symmetry B state (center), and RHR on resonance with g symmetry T state (right). Arrow lengths are not proportional to photon energies. See eq 1.

Because the B and T states are relatively close in energy, it is likely that both of the paths shown in Figure 5 contribute somewhat to the RHR scattering in both excitation ranges. Thus, it is not surprising that some of the same modes are strong under both resonance conditions. However, there are some distinct differences. For example, the lines at 1327 and 1488 cm^{-1} are among the strongest in the RHR spectrum obtained with 880 nm excitation but are quite weak at 748 nm. This suggests that these two u symmetry modes are active in coupling the one-photon forbidden T state to one or more other states that are strongly dipole-allowed from the ground state, most likely the Q and/or B states.

Tuning the RHR excitation from 748 nm to a slightly shorter wavelength (e.g., 731 nm) brings the laser fundamental closer to one-photon resonance with the Q band origin but also moves the two-photon energy farther away from the T state. Therefore, it is not obvious as to whether shortening the laser wavelength should increase or decrease the hyper-Raman intensity, and the fact that we see little effect experimentally does not allow us to evaluate the importance of the intermediate state near resonance. Previous work on a very different molecular system, in which we could tune the energy of the near-resonant one-photon state without significantly changing the two-photon resonant-state energy, indicated that moving the supposed intermediate state closer to resonance yielded no significant RHR enhancement.[11] High-level electronic structure calculations of the competing pathways involved in phthalocyanine two-photon absorption would be very helpful in interpreting these results and guiding future experiments.

Acknowledgment. This work was supported by NSF Grant CHE-0446055.

References and Notes

(1) Denisov, V. N.; Martin, B. N.; Podobedov, V. B. *Phys. Rep.* **1987**, *151*, 1.
(2) Ziegler, L. D. *J. Raman Spectrosc.* **1990**, *21*, 769.
(3) Kelley, A. M.; Leng, W.; Blanchard-Desce, M. *J. Am. Chem. Soc.* **2003**, *125*, 10520.
(4) Shoute, L. C. T.; Blanchard-Desce, M.; Kelley, A. M. *J. Chem. Phys.* **2004**, *121*, 7045.
(5) Kelley, A. M. *Int. J. Quantum Chem.* **2005**, *104*, 602.
(6) Shoute, L. C. T.; Bartholomew, G. P.; Bazan, G. C.; Kelley, A. M. *J. Chem. Phys.* **2005**, *122*, 184508.
(7) Shoute, L. C. T.; Blanchard-Desce, M.; Kelley, A. M. *J. Phys. Chem. A* **2005**, *109*, 10503.
(8) Kelley, A. M.; Shoute, L. C. T.; Blanchard-Desce, M.; Bartholomew, G. P.; Bazan, G. C. *Mol. Phys.* **2006**, *104*, 1239.
(9) Shoute, L. C. T.; Woo, H. Y.; Vak, D.; Bazan, G. C.; Kelley, A. M. *J. Chem. Phys.* **2006**, *125*, 54506.
(10) Shoute, L. C. T.; Helburn, R.; Kelley, A. M. *J. Phys. Chem. A* **2007**, *111*, 1251.
(11) Leng, W.; Kelley, A. M. *J. Chem. Phys.* **2007**, *127*, 164509.
(12) Myers, A. B. *Acc. Chem. Res.* **1997**, *30*, 519.
(13) Myers, A. B. In *Laser Techniques in Chemistry*; Myers, A. B., Rizzo, T. R., Eds.; Wiley: New York, 1995; p 325.
(14) Drobizhev, M.; Makarov, N. S.; Stepanenko, Y.; Rebane, A. *J. Chem. Phys.* **2006**, *124*, 224701.
(15) Neddersen, J. P.; Mounter, S. A.; Bostick, J. M.; Johnson, C. K. *J. Chem. Phys.* **1989**, *90*, 4719.
(16) Mack, J.; Stillman, M. J. *J. Phys. Chem.* **1995**, *99*, 7935.
(17) Nyokong, T.; Gasyna, Z.; Stillman, M. J. *Inorg. Chem.* **1987**, *26*, 1087.
(18) Van Cott, T. C.; Rose, J. L.; Misener, G. C.; Williamson, B. E.; Schrimpf, A. E.; Boyle, M. E.; Schatz, P. N. *J. Phys. Chem.* **1989**, *93*, 2999.
(19) Ricciardi, G.; Rosa, A.; Baerends, E. J. *J. Phys. Chem. A* **2001**, *105*, 5242.
(20) Ding, H.; Wang, S.; Xi, S. *J. Mol. Struct.* **1999**, *475*, 175.
(21) Tackley, D. R.; Dent, G.; Smith, W. E. *Phys. Chem. Chem. Phys.* **2000**, *2*, 3949.
(22) Liu, Z.; Zhang, X.; Zhang, Y.; Jiang, J. *Spectrochim. Acta, Part A* **2007**, *67*, 1232.
(23) Cyvin, S. J.; Rauch, J. E.; Decius, J. C. *J. Chem. Phys.* **1965**, *43*, 4083.
(24) Chung, Y. C.; Ziegler, L. D. *J. Chem. Phys.* **1988**, *88*, 7287.
(25) Bonang, C. C.; Cameron, S. M. *J. Chem. Phys.* **1992**, *97*, 5377.
(26) Ikeda, K.; Uosaki, K. *J. Phys. Chem. A* **2008**, *112*, 790.
(27) Shoute, L. C. T.; Leng, W.; Kelley, A. M., unpublished data.

JP801016Q